*Int. J. Electrochem. Sci.*, 15 **(2020)** 1082 – 1090, doi: 10.20964/2020.02.19

International Journal of
ELECTROCHEMICAL
SCIENCE
www.electrochemsci.org

# Corrosion and Discharge Performance of Mg-2Zn-0.5Ce-0.5Mn-0.2Ca Alloy in NaCl Solution

*Yanchun Zhao[1], Guangsheng Huang[2,3,*], Guangang Wang[2], Zhenghua Yao[1], Cheng Peng[1] and Fusheng Pan[2,3]*

[1] Chongqing Key Laboratory of Extraordinary Bond Engineering and Advanced Materials Technology, Yangtze Normal University, Chongqing 408100, China
[2] State Key Laboratory of Mechanical Transmission, Chongqing University, Chongqing 400044, China
[3] National Engineering Research Center for Magnesium Alloys, Chongqing University, Chongqing 400044, China
*E-mail: gshuang@cqu.edu.cn

*Received:* 4 October 2019 / *Accepted:* 18 November 2019 / *Published:* 31 December 2019

In this study, Mg-2Zn-0.5Ce-0.5Mn-0.2Ca alloy was prepared. The corrosion and discharge properties of the alloy in 3.5 wt.% NaCl solution was studied and compared with those of an AZ31 alloy. The Mg-2Zn-0.5Ce-0.5Mn-0.2Ca alloy exhibits higher corrosion resistance than that of the AZ31 alloy. The corrosion current densities of the Mg-2Zn-0.5Ce-0.5Mn-0.2Ca and AZ31 alloys are 0.31 mA $cm^2$ and 0.54 mA $cm^2$, respectively. The Mg-2Zn-0.5Ce-0.5Mn-0.2Ca alloy also exhibits better discharging performance, such as a higher discharge voltage and anodic efficiency, than that of the AZ31 alloy. The average discharge potentials of the Mg-2Zn-0.5Ce-0.5Mn-0.2Ca and AZ31 anodes are -1.45 V and -1.31 V mA $cm^2$, respectively. The anodic efficiencies of the Mg-2Zn-0.5Ce-0.5Mn-0.2Ca and AZ31 anodes are 62.1% and 53.8%, respectively. Thus, the Mg-2Zn-0.5Ce-0.5Mn-0.2Ca alloy is a good candidate as an anode material for Mg batteries.

**Keywords:** Mg-2Zn-0.5Ce-0.5Mn-0.2Ca alloy; Corrosion resistance; Discharge potential; Anodic efficiency

## 1. INTRODUCTION

A shortage of energy and an increase in environmental pollution are restricting and affecting daily life, so the development and use of green energy is urgent [1, 2]. Mg batteries, e.g., Mg-air batteries, Mg seawater-activated batteries and magnesium dry cells, are good candidates for green energy applications because they contribute no pollution and have a high energy density, low cost and wide availability [3-6]. However, Mg alloys easily corrode due to their negative standard electrode

potential. Thus, Mg anodes have a low utilization efficiency during the discharge process, which has seriously set back the development of Mg batteries seriously [7, 8].

Many studies have shown that an alloying treatment is an efficient way to enhance the corrosion resistance and discharge performance of Mg alloys [9-11]. The common alloying elements include aluminium, zinc, lithium, manganese, calcium, zirconium, lead and rare earth elements. An AP65 (Mg-6 wt.% Al-5 wt.% Pb) alloy exhibited superior discharge performance. However, Pb is harmful to human bodies. An AZ31 alloy shows excellent overall performance, which is frequently used as an anode material for Mg batteries in commercial products. Furthermore, Zinc is one of the essential elements of the human body. Recently, many studies have shown that a Mg-Zn alloy doped with appropriate minor alloying elements has a high corrosion resistance [5, 6]. Rosalbino et al. [6] examined the corrosion performance of Mg-2Zn-0.2X (X = Ca, Mn, Si) alloys and compared it with that of an AZ91 alloy in a simulated body fluid. The results show that the Mg-2Zn-0.2Mn alloy has a superior corrosion resistance, which is much higher than that of the AZ91 alloy. Li et al. [5] investigated the microstructure and corrosion performance of a Mg-1.5Zn-0.6Zr alloy. The Mg-1.5Zn-0.6Zr alloy shows a homogeneous single-phase structure and high corrosion resistance. The corrosion rate of the Mg-1.5Zn-0.6Zr alloy was only half that of an AZ91 D alloy in a 5 wt.% NaCl solution. Thus, a Mg-Zn alloy with an appropriate addition of alloying elements may be a good candidate as anode material for Mg batteries. However, the discharge performance of Mg-Zn-based alloys has rarely been reported.

In this study, Ca, Ce, and Mn are used as alloying elements, and a Mg-2Zn-0.5Ce-0.5Mn-0.2Ca alloy is prepared. The corrosion and discharge performance of the alloy is investigated using electrochemical methods. An AZ31 alloy is chosen as the contrast. The purpose of this work is to find a superior Mg anode for a magnesium-based primary battery, which has no harmful effect to human bodies or the environment.

## 2. EXPERIENTIAL

Mg alloy with a nominal composition of Mg-2Zn-0.5Ce-0.5Mn-0.2Ca was prepared from ingots of pure magnesium (99.995 wt.%), pure zinc (99.995 wt.%), Mg-10 wt.% Ce, Mg-5 wt.% Mn, and Mg-10 wt.% Ca intermediate alloys using a medium frequency induction furnace under a cover gas mixture of $CO_2$ and $SF_6$. The obtained ingot was homogenized at 420°C for 6 h. Then, the alloy was extruded at 350°C and subsequently rolled at 300°C. Finally, the rolled alloy was annealed at 400°C for 6 h to eliminate any defects. The actual chemical composition (wt.%) of the alloy was as follows: 1.99 Zn, 0.45 Ce, 0.42 Mn, 0.18 Ca and Mg balance. Commercially rolled AZ31 alloy was used for comparison, which had the following chemical composition (wt.%): 2.75 Al, 0.91 Zn, 0.31 Mn, 0.15 Si and Mg balance.

A three-electrode electrochemical cell was used to measure the polarization curves and electrochemical impedance spectra (EIS) of the alloys. A platinum plate with a size of 15 mm×15 mm was used as the counter electrode. A saturated calomel electrode (SCE) was used as the reference electrode. Test samples with a size of 10 mm×10 mm were used as the working electrodes. The surface

of the test samples was ground with 1200-grit SiC paper. A 3.5 wt.% NaCl solution prepared from distilled water and analytical grade NaCl was employed as the electrolyte.

Polarization curves were performed at a scan rate of 1 mV $s^{-1}$, while the EIS curves were performed at the OCP potential from 100 KHz to 0.1 Hz. The potential-time curves were performed at an anodic current density of 10 mA $cm^{-2}$. All the electrochemical measurements were performed at 25±1°C after a 30 min immersion of the samples, and a PGSTAT 302N system was used for the measurements. The EIS curves were fitted with ZSimpWin software. The utilization efficiency of the Mg anodes was calculated by the following equation [12-14]:

$$\text{Anodic efficiency}\ (\%) = \frac{i \times A \times t \times M_a}{2F \times (W_i - W_f)} \times 100\% \qquad (1)$$

where i represents the current density (A $cm^{-2}$), A represents the surface area of the anode ($cm^2$), t represents the total discharging time (h), Ma represents the atomic mass (g $mol^{-1}$) of the anode, F represents the Faraday constant (96485 C $mol^{-1}$), and $W_i$ and $W_f$ represent the weights of the Mg anodes before and after the discharging test, respectively. The surface morphologies of the discharge products were examined using a TESCAN VEGA-3 LMH scanning electron microscopy (SEM) system.

## 3. RESULTS AND DISCUSSION

Fig. 1 shows the metallographic structure of the Mg-2Zn-0.5Ce-0.5Mn-0.2Ca and AZ31 alloy. The Mg-2Zn-0.5Ce-0.5Mn-0.2Ca alloy exhibits a much finer grain size compared with that of the AZ31 alloy. The reason is that the Ca, Ce and Mn elements play a role as grain refiners during solidification of the alloy.

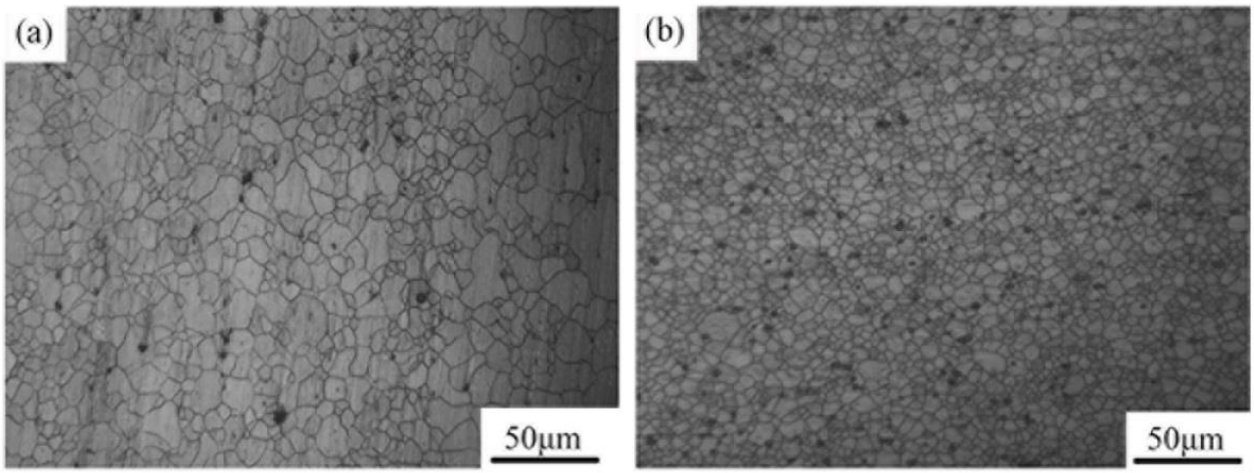


**Figure 1.** Metallographic structure of the (a) AZ31 and (b) Mg-2Zn-0.5Ce-0.5Mn-0.2Ca alloys.

Fig. 2 shows the polarization curves of the Mg-2Zn-0.5Ce-0.5Mn-0.2Ca and AZ31 alloys in 3.5 wt.% NaCl solution. The corrosion potential (Ecorr) and corrosion current density (Icorr) values corresponding to the polarization curves from Fig. 2 are listed in Table 1.

**Table 1.** Corrosion parameters of the Mg-2Zn-0.5Ce-0.5Mn-0.2Ca and AZ31 alloys.

| Samples | Ecorr (V) | Icorr (mA $cm^{-2}$) |
|---|---|---|
| Mg-2Zn-0.5Ce-0.5Mn-0.2Ca | -1.62 | 0.31 |
| AZ31 | -1.58 | 0.54 |

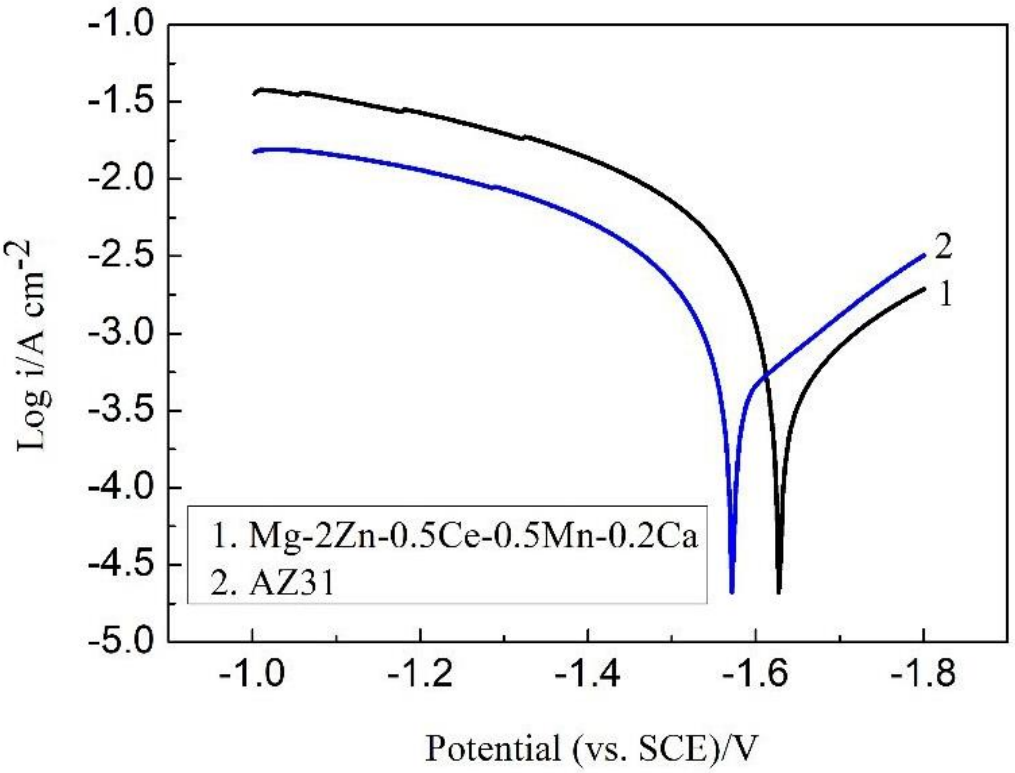


**Figure 2.** Polarization curves of Mg-2Zn-0.5Ce-0.5Mn-0.2Ca and AZ31 alloy in 3.5 wt.% NaCl solution.

The two curves are similar in shape, indicating that the two alloys have similar corrosion mechanisms. However, the Mg-2Zn-0.5Ce-0.5Mn-0.2Ca alloy exhibits a higher corrosion resistance compared with that of the AZ31 alloy. The corrosion current densities of the Mg-2Zn-0.5Ce-0.5Mn-0.2Ca and AZ31 alloys were 0.31 and 0.54 mA $cm^{-2}$, respectively. There are two reasons for the higher corrosion resistance of the Mg-2Zn-0.5Ce-0.5Mn-0.2Ca alloy. On the one hand, the finer grain size of the Mg-2Zn-0.5Ce-0.5Mn-0.2Ca alloy can provide more grain boundaries that can act as physical barriers during the corrosion process. Moreover, it has been widely reported that the addition of Ca and Ce in a Mg alloy can provide a protective corrosion product film. This product film can hinder further corrosion of the alloy during the corrosion process [15, 16]. Moreover, the Mg-2Zn-0.5Ce-0.5Mn-0.2Ca alloy shows higher electrochemical activity than that of the AZ31 alloy. The corrosion potentials of the Mg-2Zn-0.5Ce-0.5Mn-0.2Ca and AZ31 alloys are -1.62 V and -1.58 V, respectively. The reason is that grain boundaries can improve the electrochemical activity of a Mg alloy, and the Mg-2Zn-0.5Ce-0.5Mn-0.2Ca alloy can provide more grain boundaries.

Fig. 3 shows the EIS curves of the Mg-2Zn-0.5Ce-0.5Mn-0.2Ca and AZ31 alloys in a 3.5 wt.% NaCl solution. The Nyquist plot for the Mg-2Zn-0.5Ce-0.5Mn-0.2Ca alloy consist of two capacitive loops and an inductive loop. The capacitive loop in the high frequency region is related to the charge transfer process, and the second capacitive loop is attributed to the product film on the alloy surface, whereas the inductive loop is caused by a metastable $Mg^+$ concentration [17-19]. However, the AZ31 alloy only consists of a frequency capacitive loop and an inductive loop. The capacitive loop and inductive loop were attributed to the charge transfer process and metastable $Mg^+$ concentration, respectively [17, 18]. The absence of the second loop for the AZ31 alloy indicates that the corrosion products provide weaker protection to corrosion compared with that of the Mg-2Zn-0.5Ce-0.5Mn-0.2Ca alloy. The equivalent circuits of the EIS curves are shown in Fig. 4. $R_s$ is the solution resistance, CPE is the constant phase element used to replace an ideal capacitor, $CPE_{dl}$ is the double layer capacitance between the alloy surface and the solution, $R_t$ is the charge-transfer resistance, $CPE_f$ and $R_f$ are the constant phase element and resistance for the product film, respectively, and $R_l$ and L represent the resistance and inductance of the inductive loop, respectively. The EIS results are fitted by ZSimpWin software and shown in Table 2.

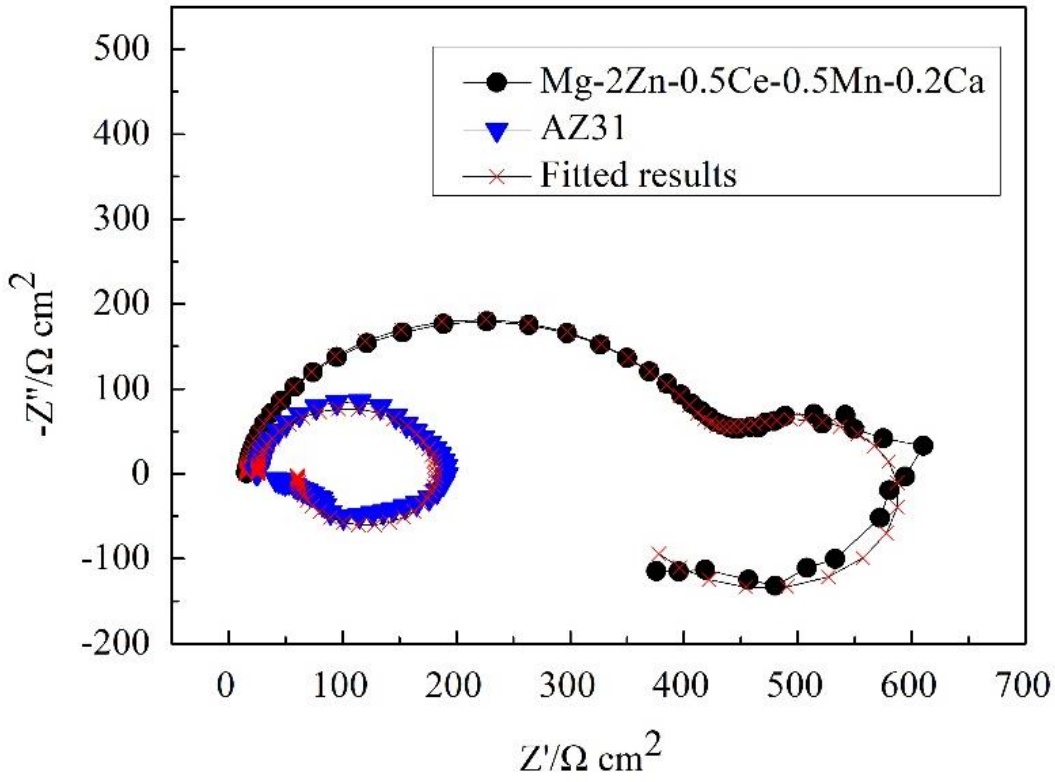


**Figure 3.** Electrochemical impedance spectra of the Mg-2Zn-0.5Ce-0.5Mn-0.2Ca and AZ31 alloys in a 3.5 wt.% NaCl solution.

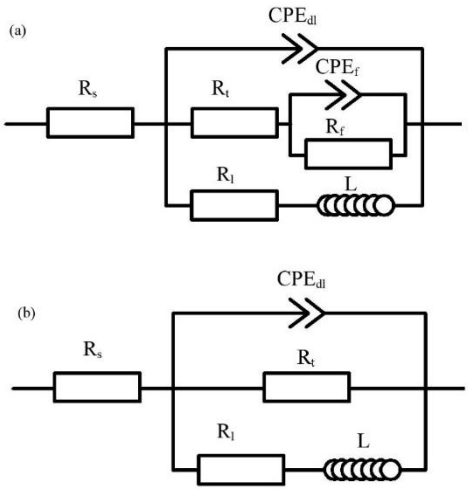


**Figure 4.** Equivalent circuits of the EIS curves: (a) Mg-2Zn-0.5Ce-0.5Mn-0.2Ca and (b) AZ31.

**Table 2.** Fitting results for the EIS curves.

| Samples | $R_s$ ($\Omega$ cm$^2$) | $Y_{dl}$ ($\Omega^{-1}$ cm$^{-2}$ s$^{-1}$) | $n_{dl}$ | $R_t$ ($\Omega$ cm$^2$) | $Y_f$ ($\Omega^{-1}$ cm$^{-2}$ s$^{-1}$) |
|---|---|---|---|---|---|
| Mg-2Zn-0.5Ce-0.5Mn-0.2Ca | 15.41 | 1.39x10-5 | 0.93 | 403.9 | 4.07x10-3 |
| AZ31 | 25.46 | 1.22x10-5 | 0.99 | 156.8 | |
| Samples | $n_f$ | $R_f$ ($\Omega$ cm$^2$) | $R_l$ ($\Omega$ cm$^2$) | L (H cm$^{-2}$) | |
| Mg-2Zn-0.5Ce-0.5Mn-0.2Ca | 0.687 | 284.1 | 622.3 | 6953 | |
| AZ31 | | | 45.11 | 44.62 | |

As shown in Table 2, the Mg-2Zn-0.5Ce-0.5Mn-0.2Ca alloy shows a much higher corrosion resistance compared with that of the AZ31 alloy. The $R_t$ values for the Mg-2Zn-0.5Ce-0.5Mn-0.2Ca and AZ31 alloys are 403.9 and 156.8 $\Omega$ cm$^2$, respectively. The EIS results are highly consistent with the potentiodynamic polarization results.

The potential-time curves of the Mg-2Zn-0.5Ce-0.5Mn-0.2Ca and AZ31 alloys at a current density of 10 mA cm$^{-2}$ are shown in Fig. 5. The Mg-2Zn-0.5Ce-0.5Mn-0.2Ca alloy exhibits a higher discharge potential compared with that of the AZ31 alloy. The average discharge potentials of the Mg-2Zn-0.5Ce-0.5Mn-0.2Ca and AZ31 alloys are -1.45 V and -1.31 V, respectively. The high electrochemical activity of the Mg-2Zn-0.5Ce-0.5Mn-0.2Ca alloy is one of the reasons for its high discharge potential. The anode efficiencies of the two alloys are shown in Fig. 6. The anode efficiency of Mg-2Zn-0.5Ce-0.5Mn-0.2Ca (62.1%) is much higher than that of AZ31 alloy (53.8%). Obviously, the higher anode efficiency of the Mg-2Zn-0.5Ce-0.5Mn-0.2Ca alloy results from its high corrosion resistance. AP65 alloy is also considered a promising anode for Mg batteries except for AZ31 alloy. According to the reported studies, the average discharge potential of the AP65 alloy is -1.76 V at 10 mA cm$^{-2}$ [20], which is higher than that of the Mg-2Zn-0.5Ce-0.5Mn-0.2Ca alloy. However, the anode efficiency of the Mg-2Zn-0.5Ce-0.5Mn-0.2Ca alloy is much higher than that of the Ap65 alloy (47%). Moreover, the Mg-2Zn-0.5Ce-0.5Mn-0.2Ca alloy is much more environmentally friendly than that of the AP65 alloy.

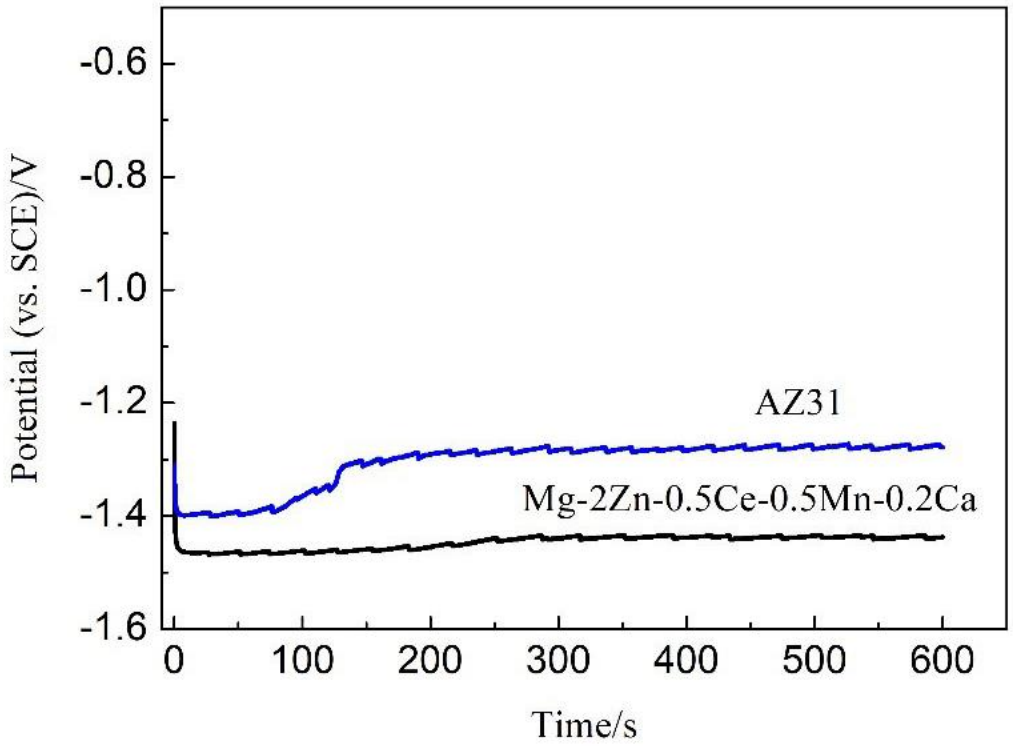


**Figure 5.** Potential-time curves of the Mg-2Zn-0.5Ce-0.5Mn-0.2Ca and AZ31 alloys in a 3.5 wt.% NaCl solution.

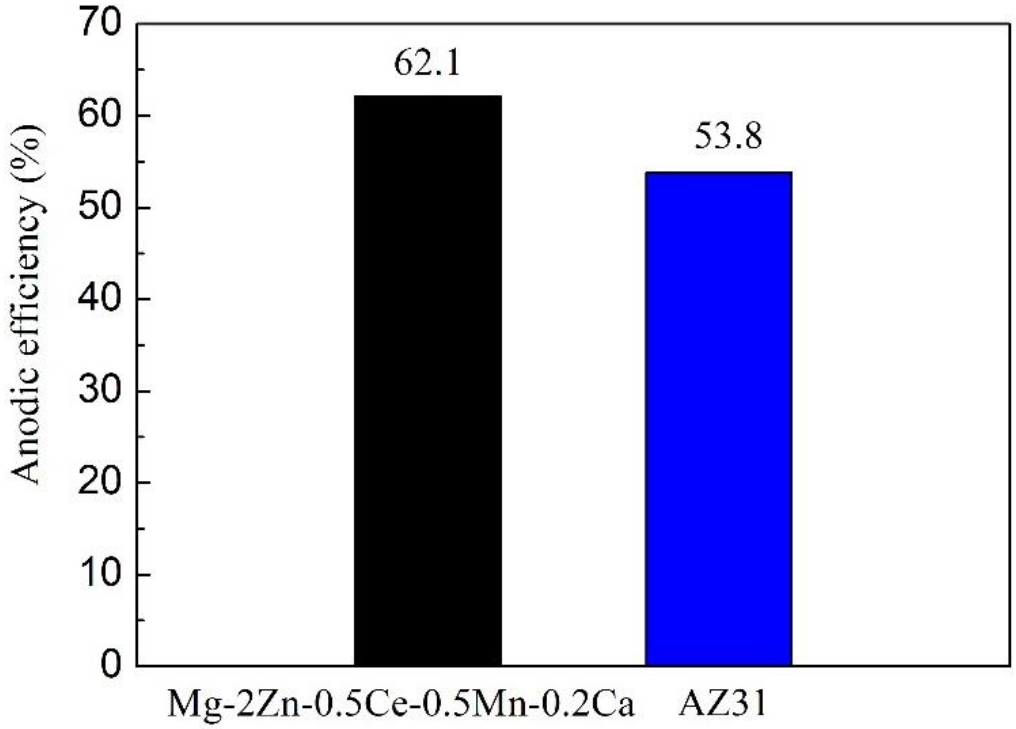


**Figure 6.** Anodic efficiency of the Mg-2Zn-0.5Ce-0.5Mn-0.2Ca and AZ31 alloys in a 3.5 wt.% NaCl solution.

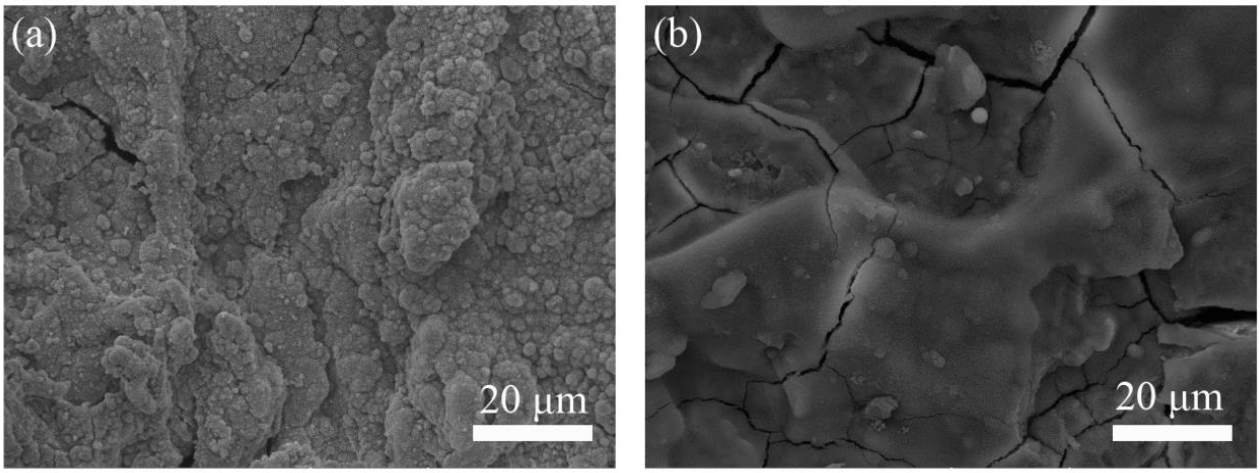


**Figure 7.** Surface morphologies of the (a) AZ31 and (b) Mg-2Zn-0.5Ce-0.5Mn-0.2Ca anodes after a discharge for 600 seconds.

The surface morphologies of the two alloys after a discharge for 600 seconds are shown in Fig. 7. The discharge product film of the Mg-2Zn-0.5Ce-0.5Mn-0.2Ca alloy is very thin and full of cracks. However, the AZ31 alloy shows a relatively think and dense product film. It has been confirmed that a loose and porous product film during discharging allows the electrolyte to pass through easily and thus enhances the discharging performance [21, 22]. Therefore, the loosely packed product film during discharging of the Mg-2Zn-0.5Ce-0.5Mn-0.2Ca alloy also enhances its discharge potential.

## 4. CONCLUSION

The corrosion and electrochemical performance of the Mg-2Zn-0.5Ce-0.5Mn-0.2Ca alloy was investigated and compared with that of the AZ31 alloy, and the results are as follows:

1) The Mg-2Zn-0.5Ce-0.5Mn-0.2Ca alloy exhibits a high corrosion resistance and electrochemical activity, which is mainly related to its fine grain size.

2) The Mg-2Zn-0.5Ce-0.5Mn-0.2Ca alloy shows a high discharge potential and anodic efficiency, mainly due to its high electrochemical activity and corrosion resistance.

3) The Mg-2Zn-0.5Ce-0.5Mn-0.2Ca alloy has a thin and loosely packed product film during discharging , while the AZ31 alloy shows a relatively think and dense product film.

ACKNOWLEDGEMENTS
This work is supported by a key project of the National Natural Science Foundation of China (No. 51531002), the Science and Technology Planning Project of the Fuling Technology Committee (FLKW, 2017ABA1018) and the Science and Technology Research Project of the Chongqing Education Commission (KJCQ201801419).

## References

1. B. Aksanli, J. Venkatesh, L. Zhang, T. Rosing, *Acm Sigops Operating Systems Review*, 45 (2012)

53.
2. L. Wang, Y. Wang, H. Yuan, *Journal of Materials Science & Technology*, 17 (2001) 590.
3. L. Xuan, S. Liu, J. Xue, *Journal of Power Sources*, 396 (2018) 667.
4. Y. Shi, C. Peng, F. Yan, R. Wang, N. Wang, *Materials & Design*, 124 (2017) 24.
5. T. Li, H. Zhang, Y. He, X. Wang, *Materials & Corrosion*, 66 (2015) 7.
6. F. Rosalbino, S.D. Negri, A. Saccone, E. Angelini, S. Delfino, *J Mater Sci Mater Med*, 21 (2010) 1091.
7. D. Lv, D. Tang, Y. Duan, M.L. Gordin, F. Dai, P. Zhu, J. Song, A. Manivannan, D. Wang, *Journal of Materials Chemistry* A, 2 (2014) 15488.
8. L. Chen, N. Sa, B. Key, A.K. Burrell, C. Lei, L.A. Curtiss, J.T. Vaughey, J.J. Woo, L. Hu, B. Pan, *Journal of Materials Chemistry* A, 3 (2015) 6082.
9. N. Wang, R. Wang, C. Peng, P. Bing, F. Yan, C. Hu, *Electrochimica Acta*, 149 (2014) 193.
10. Y. Lv, W. Li, Y. Li, Y. Jin, F. Jing, M.R. Yue, D. Cao, G. Wang, M. Zhang, *Ionics*, 20 (2014) 1573.
11. R.C. Wang, Q. Li, N.G. Wang, C.Q. Peng, Y. Feng, *Journal of Materials Engineering and Performance*, 27 (2018) 6552.
12. Y. Zhao, G Huang, C Zhang, C Peng and F Pan, *International Journal of Electrochemical Science*, 13 (2018) 8953.
13. D. Cao, C. Xue, G. Wang, W. Lin, Z. Li, *Journal of Solid State Electrochemistry*, 14 (2010) 851.
14. H. Xiong, K. Yu, Y. Xiang, Y. Dai, Y. Yang, H. Zhu, *Journal of Alloys & Compounds*, 708 (2016) 652.
15. C. Zhang, L. Wu, G. Huang, K. Liu, B. Jiang, G. Wang, D. Xia, A. Atrens, F. Pan, *Journal of The Electrochemical Society*, 166 (2019) C445.
16. J. Yang, J. Peng, E.A. Nyberg, F.-s. Pan, *Applied Surface Science*, 369 (2016) 92.
17. J. Li, Q. Jiang, H. Sun, Y. Li, *Corrosion Science*, 111 (2016) 288.
18. Y. Feng, W. Xiong, J. Zhang, R. Wang, N. Wang, *Journal of Materials Chemistry* A, 4 (2016) 8658.
19. M. Jamesh, S. Kumar, T.S. Narayanan, *Corrosion Science*, 53 (2011) 645.
20. N. Wang, R. Wang, C. Peng, Y. Feng, *Corrosion Science*, 81 (2011) 85.
21. F.E.-T. Heakal, A.M. Fekry, M.Z. Fatayerji, *Journal of applied electrochemistry*, 39 (2009) 1633.
22. Y. Ma, N. Li, D. Li, M. Zhang, X. Huang, *Journal of Power Sources*, 196 (2011) 2346.

© 2020 The Authors. Published by ESG (www.electrochemsci.org). This article is an open access article distributed under the terms and conditions of the Creative Commons Attribution license (http://creativecommons.org/licenses/by/4.0/).